Journal of
Renewable Energy Research and Applications (RERA)

Vol. 5, No 2, 2024, 211-220 *DOI: 10.22044/rera.2023.12408.1180*

A New Global Maximum Power Point algorithm for Dynamic Shading Patterns of Partial Shading

V. Pankaj[1*], G. Bharat[2], J. Gaurav[1] and H. Ravi[2]

1. Poornima College of Engineering, Jaipur, India.
2. Global Institute of Technology, Jaipur, India.

Received Date 11 November 2022; Revised Date 10 January 2023; Accepted Date 21 June 2023
**Corresponding author: pankaj.verma@poornima.org (V. Pankaj)*

Abstract
Most of the partial shading maximum power point tracking methods have been designed for the static shading pattern of the partial shading conditions; however, the irradiance pattern may change further when in partial shading mode. Therefore, to cover this research gap, a global maximum power point control under varying irradiance (GCVI) algorithm is proposed in this paper. The algorithm does not use any sensors to detect the change in the irradiance; instead, the change in the current values of the modules are continuously monitored to detect the change. The reference voltages across which the peaks on the power curve are scanned are obtained from the reference voltage generation process; the consideration of these reference points avoids the excessive power losses in the system. The verification of the working of the proposed algorithm is carried out by simulating the photo-voltaic system model on SIMULINK in the MATLAB software. Simulations are carried out in various scenarios to show the effectiveness of the control. The simulation results illustrate that with the change in the global maximum under partial shading, the system successfully retunes to the new maximum point; the maximum point retunes from 10 kW to 9.2 kW and from 13.8 kW to 11.5 kW for two different case scenarios. Further, the comparisons are also carried out with the previously reported methods.

Keywords: *Partial shading, photovoltaics, GCVI, MPPT.*

1. Introduction

The maximum power point tracking (MPPT) methods in photovoltaics (PV) aids in extracting the maximum power from the PV array. These techniques vary for uniform shading (US) and partial shading (PS) conditions; in US, PVs exhibits only a single peak, whereas, in PS, there are multiple peaks on the power *vs.* voltage (*P*-*V*) curve. MPPT techniques for uniform shading vary based on the requirement of sensors, traction time, hardware required, and operating range [1]. A detailed comparison of MPPT technique with their limitations is given in [2]. The very popular incremental conductance algorithm was discussed in [3]. The fractional open circuit voltage method in which the maximum power point (MPP) voltages are assumed as a fraction of open circuit voltage was discussed in [4, 5]. An offline look-up table technique to track the MPP in PVs was elaborated in [6]. One of interesting fuzzy logic based techniques where the fuzzy logic is used to reach the MPPT is discussed in [7]. In [8],Kennedy and Eberhart have discussed the particle swarm optimization based MPPT algorithm.

The above methods have discussed the MPPT under US conditions; however, US is not possible all time, depending upon the climatic conditions or irradiance pattern; the shading may change to PS. The following techniques have explained the MPPT under PS conditions.

[9] has introduced an improved genetic algorithm to track MPP under PS. A cuckoo search-based MPPT technique with some outstanding features and properties was introduced in [10]. An Ant Colony Optimization wherein the convergence is independent from initial location of the sample was discussed in [11]. The authors in [12] have introduced a grey wolf optimization in which the collective hunting mechanism of grey wolves is repeated for MPPT. [13] has introduced a butterfly optimization algorithm which is based on the inclusive behavior and food searching of butterflies. Butterfly optimization algorithm increases the MPPT speed, which is verified under three insolation scenarios in [14]. The simulation

outcomes of moth-flame optimization [15] unfolds that the methods can perform better than other methods like incremental conductance, fuzzy logic control, and particle swarm optimization with respect to steady state tracking ability and efficiency. Whale optimization algorithm which is the specialized hunting process of humpback whale was employed for MPPT under PS in [16, 17]. A modified firefly algorithm for MPPT during PS was introduced in [18]. A salp swarm algorithm which imitates the peerless swarm food manhunt behavior of salps was discussed in [19], whereas a modified mimic salp swarm algorithm for improved search capability and fast convergence was introduced in [20]. Similarly, [21] has introduced a chicken swarm optimization technique and the improved chicken swarm optimization algorithm was presented in [22]. The flower pollination algorithm having a good convergence rate is discussed in [23]. Authors in [24] have introduced a cat swarm optimization. A simulated annealing and an enhanced simulated annealing algorithm for various MPPT problems in *P-V* curves of PVs are explained in [24] and [25], respectively. In [26], a gravitational search algorithm was discussed; the ability of global searching of gravitational search algorithm is good as compared to some other heuristic algorithms like particle swarm optimization. In [27], the authors have introduced a wind driven optimization algorithm, which is basically based on the motion of atmosphere. The technique of [28] has discussed an assorted algorithm of whale optimization; this technique is based on the humpback hunting behavior of whales. An artificial neural network-sequential Monte Carlo method which is the combination of neural network and meta-heuristic algorithm was coined in [29]. For increasing the overall efficiency of the system, an improved genetic-firefly algorithm which is the combination of genetic algorithm and firefly algorithm was developed in [30]. The modifications in the traditional P&O algorithm to trace the MPP under multi-peak environment were carried out in [31].

There are enormous methods available in the literature for MPP tracking under uniform shading and partial shading conditions. Many methods have been reviewed above, however, the focus of this paper is on the methods dealing with the MPPT under partial shading conditions. The notable research gaps of the surveyed methods are as follow: (1) In many control schemes, there is no parameter to detect the change in irradiance further after the onset of the partial shading conditions. The shading pattern of the irradiance may change from one to another, there should be a control to detect this change. (2) Under partial shading conditions, the irradiance may change further and the location of maxima can alter on the power versus voltage curve of PVs. Many of the methods have been designed only for the static partial shading conditions, the further possible change has been ignored in these methods. A comparison of these methods with the purposed technique is given in table1. Based upon the mentioned research gaps, the main objectives of this paper are as follow:

a) To develop an efficient maximum power point tracking method for partial shading condition of photovoltaic with the help of voltage reference scanning control.

b) To detect the further change in irradiance pattern under partial shading conditions and hunt the new global maximum power point.

c) To compare the developed method with already proposed methods to illustrate the merits of the proposed control.

2. Overview of research problem

When all the panels of an array receive the same irradiance level, the *P-V* curve consists of a single peak or maximum; however, upon an change in the irradiance levels of the modules of the same array, the number of peaks on the *P-V* curve increases, thus the problem changes to hunting the global maximum of the two available peaks. The number of peaks mostly depends upon the number of irradiance levels. Many methods are available in the literature, which perform the MPPT under partial shading conditions, but these methods do not address the situation where the irradiance levels on modules changes further. Under this scenario, the position, number, power level of peaks may change.

Three such scenarios are considered here to generate the understanding for two peak *P-V* curve of PVs. In scenario 1, initially the right peak is the global maximum power point (GMPP) and left peak is the local maximum power point (LMPP); the irradiance in the system may change in such a manner that the P-V curve may shrink and the position/power level of GMPP may fall down as shown in figure 1. In this figure, the initial GMPP is GMPP1 and the final GMPP is GMPP2, the initial curve is shown in black, colour and the final curve is shown in red colour, whereas the position of the LMPP remain fixed in this case

Table 1. Comparison of PS MPPT methods.

Algorithm	Complexity	Sensor used	Expenditure	PV module dependency	Converter type	Type of shading considered	Year
Modified Genetic Algorithm [9]	Medium	I, V	High	No	Buck-Boost	Static	2014
Cuckoo Search [10]	Medium	I, V	Medium	--	Boost	Static	2014
Ant Colony Optimization [11]	Low	I, V	Medium	No	Boost	Static	2013
Enhance Grey Wolves Optimization [12]	High	I, V	High	No	Boost	Static	2017
Butterfly Optimization Algorithm [14]	Medium	I, V	Medium	No	Boost	Static	2019
Moth-Flame Optimization [15]	Medium	I, V	Medium	No	Boost	Static	2018
Whale Optimization Algorithm [16,17]	Medium	I, V	High	No	Boost	Static	2016
Modified Firefly Algorithm [18]	Medium	I, V	Medium	No	Boost	Static	2018
Modified Salp Swarm Algorithm [20]	Medium	I, V	High	No	Boost	Static	2019
Improved Chicken Swarm Optimization [22]	High	I, V	Medium	No	Boost	Static	2019
Modified Flower Pollination Algorithm [23]	Medium	I, V	High	No	Boost	Static	2018
Simulated Annealing [25]	High	I, V	Low	Yes	Boost	Static	2015
Improved Gravitational Search Algorithm [26]	High	I, V	Medium	No	Boost	Static	2018
Wind-driven Optimization [27]	Low	I, V	High	No	Boost	Static	2018
Whale Optimization Algorithm and Differential Evolution [28]	High	I, V, P	High	Yes	N.P.	Static	2017
Artificial Neural Network-Sequential Monte Carlo [29]	High	I, V	Very High	No	N.P.	Static	2019
Improved Genetic Algorithm and Firefly Algorithm [30]	Medium	I, V	Medium	Yes	Buck	Static	2018
Proposed method	Low	I,V	Low	No	Boost	Dynamic	--

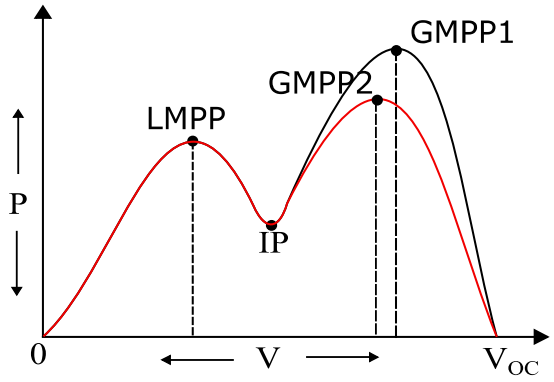

Figure 1. Depiction of scenario 1.

In scenario 2, initially the left peak is the GMPP and right peak is the LMPP; the irradiance in the system may change in such a manner that the P-V curve may shrink and the position/power level of GMPP may fall down as shown in figure 2. In this figure, the initial GMPP is GMPP1 and the final GMPP is GMPP2; the initial curve is shown in black colour, and the final curve is shown in red colour, whereas the position of the LMPP remain fixed for this case also. The IP is called the inflection point; this is the point where one peak ends and the other one starts.

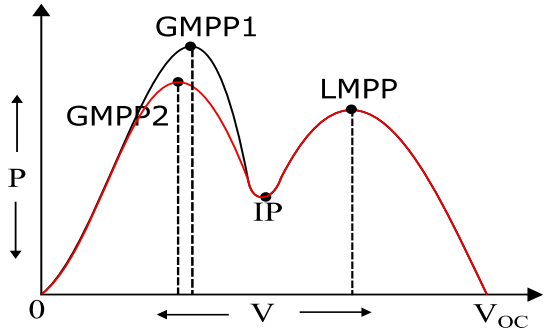

Figure 2. Depiction of scenario 2.

For scenario 3, initially the left hand side peak is the GMPP and right hand side peak is the LMPP; the irradiance in the system may change in such a manner that the *P-V* curve may expand and the position of the GMPP changes from left side to right side and the power level of GMPP increases as shown in figure 3. In this scenario, the initial GMPP, i.e. GMPP1 now becomes the LMPP and the current GMPP is at the position of GMPP2. The initial curve is shown in black colour, and the final curve is shown in red colour. For the effective working of the MPPT algorithms under these depicted PS conditions, the algorithm must track the new GMPPs. The tracking depends upon the set parameters and the technique opted for scanning.

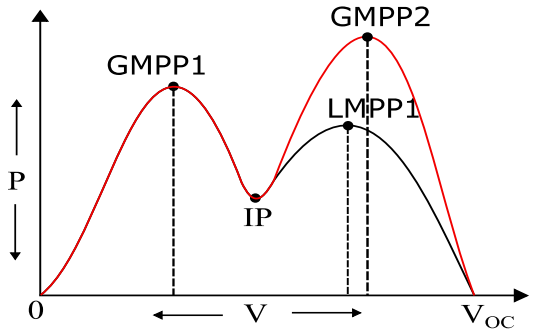

Figure 3. Depiction of scenario 3.

3. Global maximum power point control under varying irradiance (GCVI)

The complete structure and application of the proposed GCVI algorithm on the PV system is explained in this section; however, before explaining this control, the explanation of few concepts is essential to generate a proper understanding of the algorithm. Therefore, the section is divided into sub-sections: Section 3.1 discusses the reference voltage generation process, Section 3.2 explains the function of back diode under PS, and Section 3.3 discusses the GCVI algorithm

3.1. Reference voltage generation process

The first step in the development of GCVI algorithm is to find the reference voltages across which the *P-V* curve may be scanned to converge to the maximum (local or global) at the earliest. The whole *P-V* curve cannot be scanned to locate LMPP or GMPP, as this gives rise to increase in the power losses of the system. The proposed GCVI control is developed for only two peaks cases, in these cases, two reference voltages are needed one for the left peak and one for the right peak. The reference voltage value for left peak (V_{ref1}) is obtained using equation:

$$\mathbf{V_{ref1}} = \frac{(\mathbf{V_{SC}} + \mathbf{0.3V_{OC}})}{\mathbf{2}} \quad (1)$$

here, V_{SC} is the short circuit voltage whose value is zero and V_{OC} is the open circuit voltage; this value is normally specified on rating manuals of PVs. The left peak normally lies on the 0 to 30 % value of the V_{OC}; here, an average is used to ensure convergence. Similarly, the reference voltage for right peak (V_{ref2}) is obtained using equation:

$$\mathbf{V_{ref2}} = \frac{(\mathbf{0.7V_{OC}} + \mathbf{V_{OC}})}{\mathbf{2}} \quad (2)$$

The right peak normally lies on the 70 % to 100 % value of the V_{OC}; here again, an average is used to ensure convergence. The phenomenon is depicted in figure 4.

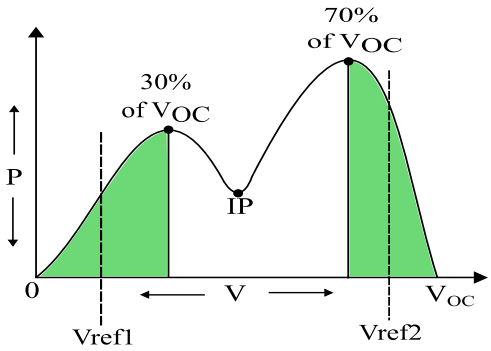

Figure 4. Reference voltage generation for two peak P-V curve.

Note: Although the developed control is only for two peaks system, however, the control can be extended to the three peaks as well; for this expansion, three reference voltages are required to complete the scan process. For this case, the V_{ref1} and V_{ref2} are computed in the same manner as in equations (1) and (2), and the third reference voltage for the middle peak (V_{ref3}) is generated using equation:

$$\mathbf{V_{ref3}} = \frac{(\mathbf{V_{ref1}} + \mathbf{V_{ref2}})}{\mathbf{2}} \quad (3)$$

Figure 5 depicts the phenomenon.

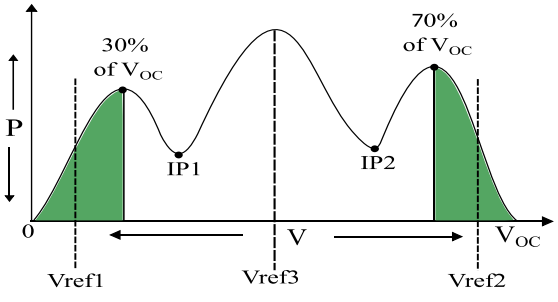

Figure 5. Reference voltage generation for three peak P-V curve.

3.2. Back-diode functionality

During the PS irradiance conditions, the modules receives the unequal irradiance levels; the shaded module receives a lower value of irradiance due to which the generated photovoltaic current of the module decreases. Consider the case of figure 6 in which the module M2 is under a lower value of irradiance due to which the value of current through this module decreases as compared to the module M1. As both the modules are connected in series configuration, the decrease in the current of one module will lead to same current value in the whole connection, therefore, to avoid this situation the back diodes are connected in anti-parallel direction which allows the additional current to flow through them. For example, let us consider the case when the series current is 10 A under uniform irradiance pattern, if the value of irradiance on module M2 changes to half of the original then the current through M2 will change to 5 A only; thus the additional series current of 5 A will pass through the back diode. In this way the current through module M1 will be maintained as 10 A.

Thus the above example depicts that the addition of back diode can help in decreasing the power losses under PS conditions by a significant amount, overall, the operation of array without back diodes under PS will result in huge amount of power loss.

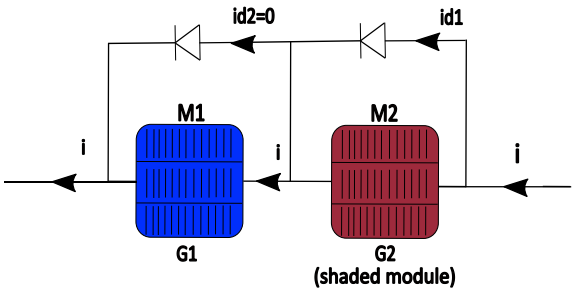

Figure 6. Partial shading condition depiction in a two module system.

3.3. GCVI algorithm

The exact implementation of the GCVI algorithm on the PV system is shown in figure 7; the algorithm block continuously senses the value of PV voltage V_{PV} and current I_{PV} to generate the reference voltages V_{ref}; these voltages are then compared with the actual V_{PV} to generate the gate pulses. Two PV modules are connected in series configuration to make an array; the ratings of these modules are given in table I of the appendix. The configuration of dc/dc converter is considered as step up/boost, the values of parameters of the converter are given in table II (appendix section). The whole system is assumed to be operating under a resistive load of 2 kW.

The detailed view of the proposed GCVI algorithm is given in figure 8; the algorithm starts by sensing the values of V_{PV} and I_{PV}, the value of V_{ref1} is set as according to equation (1), the incremental conductance (INC) algorithm is called to trace the maximum power point of the corresponding peak, i.e. the peak of left hand side. The INC tracks the MPP by observing the value of slope change on every step. After conversion, the values of power (P_{MPP1}) and voltage (V_{MPP1}) of the maximum point are stored in the system. Further, the value of V_{ref2} is set according to equation (2), the INC algorithm is called again to locate the maximum power point of the right peak, again after convergence the values of the power (P_{MPP2}) and voltage (V_{MPP2}) are stored in the system. After this scanning period, both the stored power values are compared to locate the position of GMPP. If $P_{MPP1} > P_{MPP2}$, this signifies that the GMPP lies on the left peak and V_{ref} is set as equals to V_{MPP1}, else, V_{ref} is set as equals to V_{MPP2}. The INC algorithm is called one more time to finally converge the system on the GMPP. After this step, the system keeps an close eye on the value of ΔI_{PV1} & ΔI_{PV2}, which are the change in the values of current of module 1 and module 2. Upon a further change in irradiance under PS conditions, the values of ΔI_{PV1} & ΔI_{PV2} shows a significant change, a tolerance value is used in the algorithm to detect this change; the comparison with tolerance value helps in filtering out the unwanted switching due to noise or small changes. If the values of ΔI_{PV1} & ΔI_{PV2} exceeds above the set tolerance value the scan cycle is started again so as to locate the position of new GMPP otherwise the system maintains the initial power point.

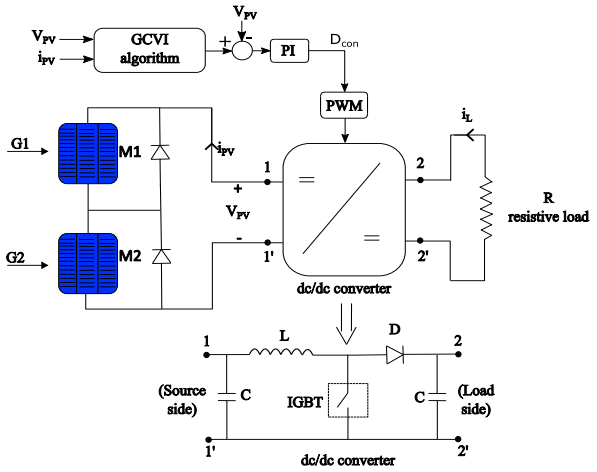

Figure 7. Implementation of GCVI control on PV system.

4. Simulation results

The simulation results of figure 7, when simulated under various irradiance conditions are given in this section. During partial shading conditions, the global maximum can arrive on the left hand side or right hand side on the power versus voltage curve (for two peak case). The simulation results for global maximum on left hand side are given in Section 4.1, and the results for global maximum on right hand side are given in Section 4.2, whereas the comparison of the proposed technique with previous works is carried out in Section 4.3**.**

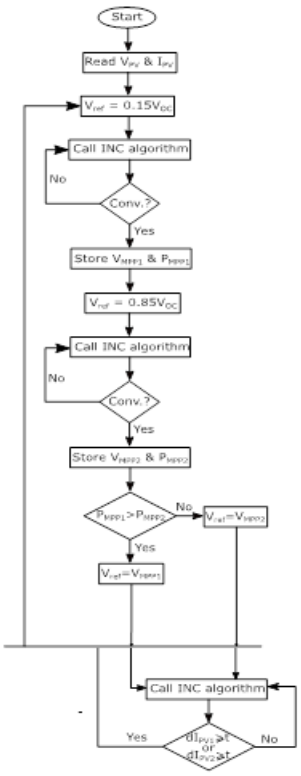

Figure 8. Detailed view of GCVI algorithm.

4.1. GCVI algorithm operation with global maximum on left hand side

The simulation results depicting the operation of GCVI with maximum on left hand side is shown in figure 9. Initially the system operates with $G_1 = 1000\,W/m^2$ & $G_2 = 300\,W/m^2$, the *P-V* curve for these values is shown in Fig. 9 (a) (bold line). The operation of the algorithm starts by first scanning the right hand side peak where a maximum power of 5650 W is recorded (Figure 9 (b)), further, the algorithm scans through the left peak with maximum power value of 10 kW, post comparisons, the algorithm converges at left peak as this peak is the global maximum. At t = 2.5 s, the irradiance levels of the modules changes to $G_1 = 900\,W/m^2$ & $G_2 = 300\,W/m^2$, due to which a dip is observed in global peak and its power value changes to 9200 W as shown in Fig. 9 (a) (dotted line). Upon change in the irradiance, the PV module currents changes drastically and the algorithm starts the scan cycle again, the PV module currents are shown in Fig. 10. The algorithm again scans the right peak and records the same power level of 5650 W, during scanning the left peak, the power level changes to 9200 W, previously this was 10 kW. However, the algorithm converges on the left peak and thus the new global maximum power point of the system is obtained.

The PV array voltage and current waveforms are given in figure 9 (c) and figure 9 (d), respectively. The right side peak is obtained at the voltage of 320 V, whereas the left side peak is obtained at the voltage of 155 V. The value of array current on the right peak is 24 A and the value on the left side peak is 65 A.

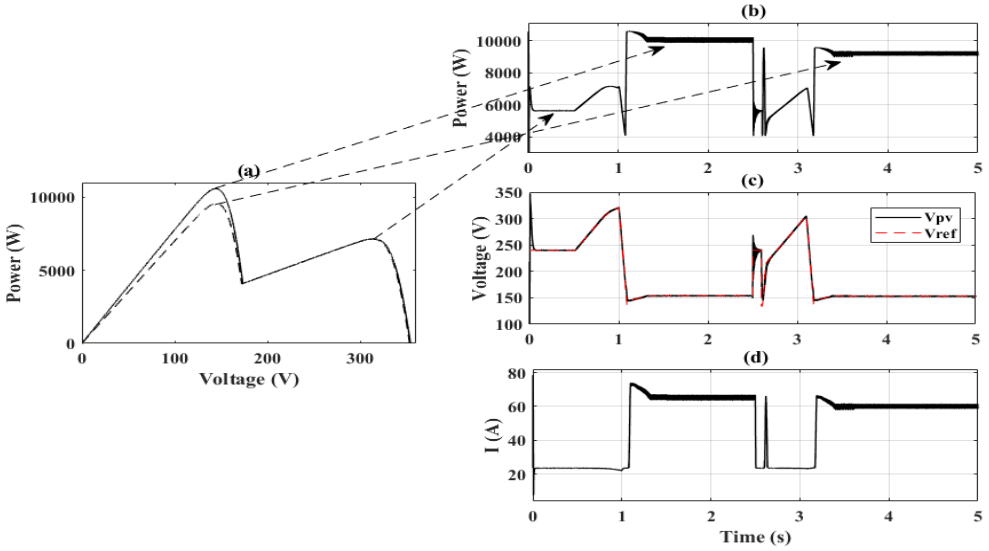

Figure 9. Simulation results with global maximum on left hand side (decrease in irradiance), (a) P-V curves, (b) PV array output power, (c) PV array voltage, and (d) PV array current.

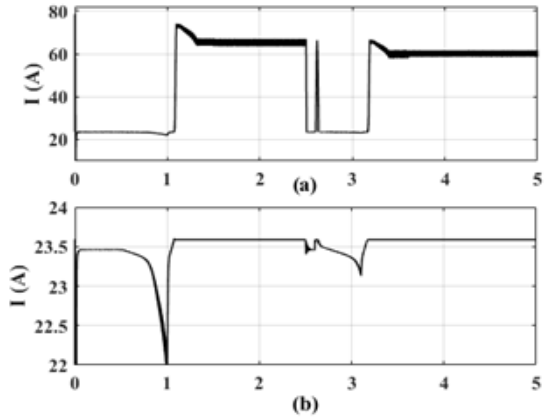

Figure 10. Simulation results with global maximum on left hand side (decrease in irradiance), (a) PV module 1 current, and (b) PV module 2 current.

4.2. GCVI algorithm operation with global maximum on right hand side

The simulation results depicting the operation of GCVI with maximum on right hand side is shown in figure 11. Initially, the system operates with $G_1 = 1000\,W/m^2$ & $G_2 = 600\,W/m^2$, the P-V curve for these values is shown in figure 11 (a) (bold line). The operation of the algorithm starts by first scanning the left hand side peak where a maximum power of 10.58 kW is recorded (Figure 11 (b)); further, the algorithm scans through the right peak with maximum power value of 13.8 kW, post comparisons, the algorithm converges at right peak as this peak is the global maximum. At t = 2.5 s, the irradiance levels of the modules changes to $G_1 = 1000\,W/m^2$ & $G_2 = 500\,W/m^2$, due to which a dip is observed in global peak and its power value changes to 11.5 kW as shown in figure 11 (a) (dotted line). Upon change in the irradiance, the PV module currents changes drastically and the algorithm starts the scan cycle again. The algorithm again scans the left peak and records the same power level of 10.58 kW, during scanning the right peak, the power level changes to 11.5 kW, previously this was 13.8 kW. However, the algorithm converges on the right peak and thus the new global maximum power point of the system is obtained.

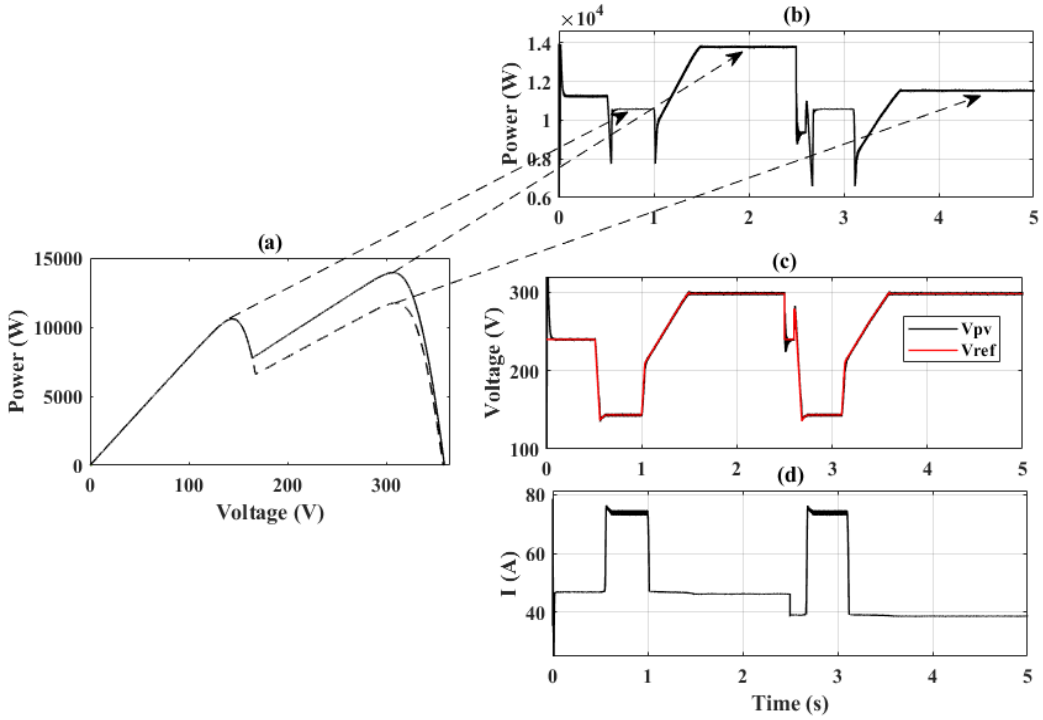

Figure 11. Simulation results with global maximum on right hand side (decrease in irradiance), (a) P-V curves, (b) PV array output power, (c) PV array voltage, and (d) PV array current.

4.3. Comparison with previous methods

The current GCVI algorithm operation is compared with the previous methods [31] in this section. The comparison is given in figure 12; the current method (CM) outputs are displayed in black colour, and the waveforms obtained from the previous methods are displayed in red colour. Initially the system operates with irradiance values as $G_1 = 1000\ W/m^2$ & $G_2 = 600\frac{W}{m^2}$; this is represented with the bold line in *P-V* curve (Figure 12 (a)), these values changes to $G_1 = 900\ W/m^2$ & $G_2 = 300\ W/m^2$ in the final state, represented with dot lines in Figure 12 (a). This change in the irradiance leads to change in the position of global peak from right side to left side.

For the operation with GCVI, the algorithm first scans through the left peak where a power level of 10 kW is recorded, further on the right peak a power level of 13.8 kW is logged by the system (Figure 12 (b)), the system finally settles on the right peak because of higher power level during comparisons. At t = 2.5 s, with the change in the irradiance as indicated above, the position of the global maximum changes towards the left hand side. Under these conditions, the left peak is scanned first where a power level of 9.2 kW is achieved, further the right peak is scanned and the recorded power level is 7.1 kW, finally the system settles on the left peak. Therefore, under the dynamic shading conditions the proposed algorithm manages to update the new global maximum power point, whereas for the operation with method of [31], after initial scan, the system settles on the right peak with power level of 13.8 kW, however, upon change in the irradiance pattern, the control fails to update the new global maximum point and converges on the right peak which is now a local maximum. The PV array voltage and current waveforms are given in figure 12 (c) and figure 12 (d), respectively.

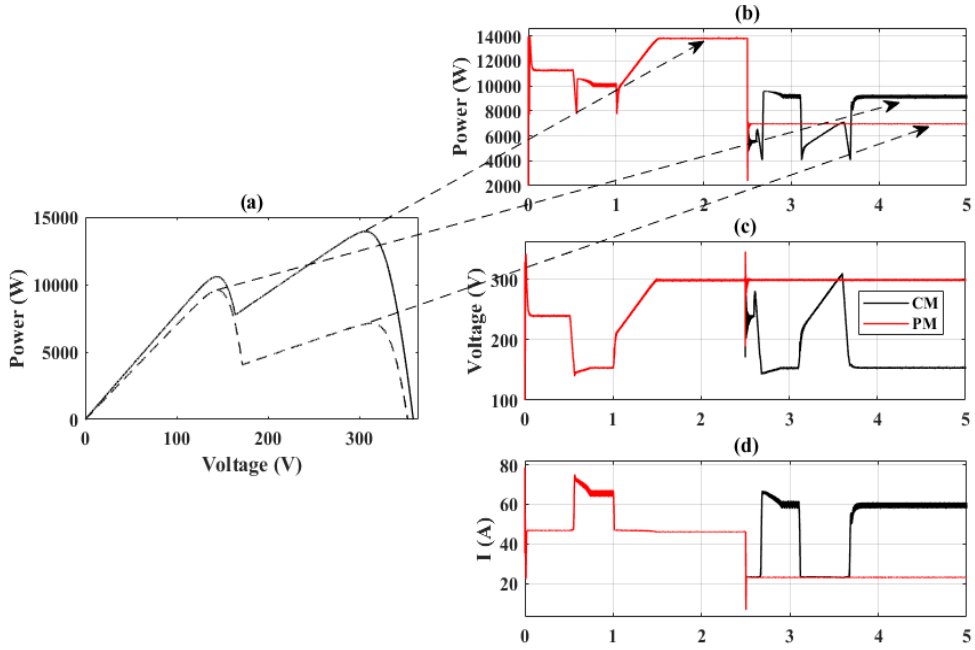

Figure, 12 Simulation results for comparison of current method with previous methods, (a) P-V curves, (b) PV array output power, (c) PV array voltage, and (d) PV array current.

5. Conclusions

In this paper, a MPPT algorithm of partial shading conditions for dynamic shading pattern, i.e. when the irradiance further changes from one pattern to other, is proposed. The algorithm avoids the power losses by scanning only across the referred voltage points for locating the global maximum. These reference voltages are generated by observing the peaks location on sample power versus voltage curve of photovoltaics and using the mean value formulas. The proposed (GCVI) algorithm effectively tracks the global maximum power point under dynamic irradiance conditions; simulation was carried out broadly under three categories for two peak *P-V* curve: (1) irradiance increase/decrease when the global peak appears on the left side, (2) irradiance increase/decrease when the global peak appears on the right side, and (3) the global peak shifts from right side to left side. Satisfactory observations were recorded. The proposed algorithm is also compared with the reported method using simulations, the results

depict that the previous methods can get trapped on the local maximum point when the position of global maximum changes from left to right or vice-versa. For future research, more number of peaks can be considered in the system and the modifications of meta-heuristic algorithms can be considered for a robust control.

6. Nomenclature

Abbreviation	Description
MPPT	The maximum power point tracking
PV	Photovoltaics
US	Uniform shading
PS	Partial shading
P-V	Power *vs.* voltage
MPP	Maximum power point
GMPP	Global maximum power point
LMPP	Local maximum power point
GCVI	Global Maximum Power Point Control under Varying Irradiance
INC	Incremental Conductance

Variable	Description
V_{ref}	Reference voltage
V_{SC}	Short-circuit voltage
V_{OC}	Open-circuit voltage
M1	Module 1
M2	Module 2
V_{PV}	PV system voltage
I_{PV}	PV system current
ΔI_{PV1}	Change in current of module 1
ΔI_{PV2}	Change in current of module 2

7. Appendix

Table I. Rating of PV modules.

	Module 1 (M1)	Module 2 (M2)
V_{OV}	182 V	182 V
I_{SC}	79 A	79 A
P_{max}	10.6 kW	10.6 kW
Temp. coefficient of V_{OV} (%/deg. C)	-0.36	-0.36
Temp. coefficient of I_{SC} (%/deg. C)	0.102	0.102

Table II. Parameters of the dc/dc converter.

Name of parameter	Value
Source side capacitor	100 µF
Inductor	5 mH
Load side capacitor	0.1 µF
Resistive load	2 kW
Switching frequency	3000 Hz
K_p (PID Controller)	0.298
K_I (PID Controller)	150.52
Diode on state resistance	0.001

8. References

[1] Dubey R, Joshi D, and Bansal RC. (2016). Optimization of Solar Photovoltaic Plant and Economic Analysis. Electr. Power Components Syst., Vol. 44, No. 5, pp. 2025-2035.

[2] Esram T and Chapman PL. (2007). Comparison of photovoltaic array maximum power point tracking techniques. IEEE Transactions on Energy Conversion, Vol. 22, No. 2, pp. 439-449.

[3] Hussein KH. (1995). Maximum photovoltaic power tracking: an algorithm for rapidly changing atmospheric conditions. IEEE Proceedings - Generation, Transmission and Distribution, Vol. 142, No. 1, pp. 59.

[4] Ahmad R, Murtaza AF, and Sher HA. (2016). Power tracking techniques for efficient operation of photovoltaic array in solar applications – a review. Renewable and Sustainable Energy Reviews, Vol. 44, No. 18, pp. 82-102.

[5] Eltamaly AM and Abdelaziz AY. (2020). Modern Maximum Power Point Tracking Techniques for Photovoltaic Energy Systems. Springer Nature, Gewerbestrasse 11, 6330 Cham, Switzerland.

[6] Bhatnagar P and Nema RK. (2017). Maximum power point tracking control techniques: state-of-the-art in photovoltaic applications. Renewable and Sustainable Energy Reviews, vol. 23, pp. 224-241.

[7] Lupangu C and Bansal RC. (2017). A review of technical issues on the development of solar photovoltaic systems. Renewable and Sustainable Energy Reviews, Vol. 73, pp. 950-965.

[8] Kennedy J and Eberhart R. (1994). Particle swarm optimization. Proceedings of International Conference on Neural Networks (ICNN), pp. 1942-1948.

[9] Tey, K.S., Mekhilef, S., Seyedmahmoudian, M., Horan, B.; Oo, A.T.; and Stojcevski (2018). A. Improved differential evolution-based MPPT algorithm using SEPIC for PV systems under partial shading conditions and load variation. IEEE Transactions on Industrial Informatics, Vol. 14, No. 10, pp. 4322-4333.

[10] Peng, B.R., Ho, K.C., and Liu, Y.H. (2018). A novel and fast MPPT method suitable for both fast changing and partially shaded conditions. IEEE Transactions on Industrial Electronics, Vol. 65, No. 4, pp. 3240-3251.

[11] Li, G.; Jin, Y., Akram, M.W., Chen, X., and Ji, J. (2018). Application of bio-inspired algorithms in maximum power point tracking for PV systems under partial shading conditions-A review. Renewable and Sustainable Energy Reviews, Vol. 81, pp. 840-873.

[12] Luo, S., Zhang, L., and Fan, Y. (2019). Energy-efficient scheduling for multi-objective flexible job shops with variable processing speeds by grey wolf optimization. Journal of Cleaner Production, Vol. 234, pp. 1365-1384.

[13] Arora, S. and Singh, S. (2019). Butterfly optimization algorithm: a novel approach for global optimization. Soft Computing, Vol. 23, No. 3, pp. 715-734.

[14] Aygül, K., Cikan, M., Demirdelen, T., and Tumay, M. (2019). Butterfly optimization algorithm based maximum power point tracking of photovoltaic systems under partial shading condition. Energy Sources, Part A: Recovery, Utilization, and Environmental Effects, vol. 19, pp. 1-19.

[15] Aouchiche, N., Aitcheikh, M.S., Becherif, M., and Ebrahim, M.A. (2018). AI-based global MPPT for partial shaded grid connected PV plant via MFO approach. Solar Energy. Vol. 171, pp. 593-603.

[16] Liu, D., Fan, Z., Fu, Q., Li, M., Faiz, M.A., Ali, S., Khan, M.I. (2019). Random forest regression evaluation model of regional flood disaster resilience based on the whale optimization algorithm. Journal of Cleaner Production, Vol. 250, 119468.

[17] Premkumar, M. and Sumithira, T.R. (2018). Humpback whale assisted hybrid maximum power point tracking algorithm for partially shaded solar photovoltaic systems. Journal of Power Electronics, Vol. 18, No. 6, pp. 1805-1818.

[18] Farzaneh, J., Keypour, R., and Khanesar, M.A. (2018). A new maximum power point tracking based on modified firefly algorithm for PV system under partial shading conditions. Technology and Economics of Smart Grids and Sustainable Energy, Vol. 3, No. 1, pp. 9-23.

[19] Krishnan, S. and Sathiyasekar, K. (2019). A novel salp swarm optimization MPP tracking algorithm for the solar photovoltaic systems under partial shading conditions. Journal of Circuits, Vol. 29, No. 1, 2050017.

[20] Yang, B., Zhong, L.E., Yu, T., Li, H.F., Zhang, X.S., Shu, H.C., Sang, Y.Y., and Jiang, L. (2019). Novel bio-inspired memetic salp swarm algorithm and application to MPPT for PV systems considering partial shading condition. Journal of Cleaner Production, Vol. 215, pp. 1203-1222.

[21] Irsalinda, N., Thobirin, A., and Wijayanti, D.E. (2017). Chicken swarm as a multi-step algorithm for global optimization. International Journal of Engineering Science Invention, Vol. 6, No. 1, pp. 8-14.

[22] Wu, Z., Yu, D., and Kang, X. (2018). Application of improved chicken swarm optimization for MPPT in photovoltaic system. Optimal Control Applications and Methods, Vol. 39, No. 2, pp. 1029-1042.

[23] Pei, T., Hao, X., and Gu, Q. (2018). A novel global maximum power point tracking strategy based on modified flower pollination algorithm for photovoltaic systems under non-uniform irradiation and temperature conditions. Energies, Vol. 11, No. 10, pp. 2708-2725.

[24] Guo, L., Meng, Z., Sun, Y., Wang, L. (2018). A modified cat swarm optimization based maximum power point tracking method for photovoltaic system under partially shaded condition. Energy, vol. 144, pp. 501-514.

[25] Wang, F., Zhu, T., Zhuo, F., Yi, H., and Fan, Y. (2017). Enhanced simulated annealing-based global MPPT for different PV systems in mismatched conditions. Journal of Power Electronics, Vol. 17, No. 5, pp. 1327-1337.

[26] Li, L.L., Lin, G.Q. Tseng, M.L., Tan, K., and Lim, M.K. (2018). A maximum power point tracking method for PV system with improved gravitational search algorithm. Applied Soft Computing, Vol. 65, pp. 338-348.

[27] Abdalla, O., Rezk, H., and Ahmed, E.M. (2019). Wind driven optimization algorithm based global MPPT for PV system under non-uniform solar irradiance. Solar Energy, Vol. 180, pp. 429-444.

[28] Kumar, N., Hussain, I., Singh, B., and Panigrahi, B.K. (2017). MPPT in dynamic condition of partially shaded PV system by using WODE technique. IEEE Transactions on Sustainable Energy, Vol. 8, No. 3, pp. 1204-1241.

[29] Chen, L. and Wang, X. (2019). Enhanced MPPT method based on ANN-assisted sequential Monte-Carlo and quickest change detection. IET Smart Grid, Vol. 2, No. 4, pp. 635-644.

[30] Huang, Y.P., Chen, X., and Ye, C.E. (2018). A hybrid maximum power point tracking approach for photovoltaic systems under partial shading conditions using a modified genetic algorithm and the firefly algorithm. International Journal of Photoenergy, Vol. 2018, 7598653.

[31] Hiren Patel and Vivek Agarwal (2008). Maximum Power Point Tracking Scheme for PV Systems Operating Under Partially Shaded Conditions. IEEE Transactions on Industrial Electronics, Vol. 55, No. 4, pp. 1689-1698.